

Simulating Water Flow into a Soil Matrix with a Cylindrical Macropore

L. Stadler, I. Martinez-Noguez & R. Hinkelmann

TU Berlin, Chair of Water Resources and Modeling of Hydrosystems, Germany

K. Germer

University of Stuttgart, Institute for Modelling Hydraulic and Environmental Systems, VEGAS, Germany

ABSTRACT: The simulation of water transfer between the soil matrix and macropores is crucial for modeling flow in macroporous soils. We present a numerical model (CASCADE) that allows to simulate the flow in a single macroporous and the water transfer between the macropore and its surrounding soil matrix. CASCADE is coupled with existing modeling software for porous media which models the flow in the soil matrix (MUFTE-UG, DuMuX). We show experimental and numerical results of two laboratory experiments. The exchange parameter is determined together with other sensitive parameters (van Genuchten parameters, permeability, residual saturation) through parameter optimization. Overall a good agreement between computations and measurements is obtained.

Keywords: Macropore flow, Infiltration, Discrete model concept, Two-phase flow in porous media, Numerical model

1 INTRODUCTION

Macropore flow is a typical phenomenon in field soils where soil fauna, flora and genesis can form a network of large soil pores. Water and solutes can shortly reach deeper soil regions via macropores while bypassing lower permeable soil layers (Beven and German, 1982). For this reason, it is challenging to predict, flow and transport processes in macroporous soils with numerical models. Today a wide range of scale and problem dependent models and concepts for simulating flow in macroporous soils exist (Simunek et al. 2003, Gerke 2006, Köhne et al. 2009). Macropore flow can be taken into account with a discrete model concept (Stadler et al. 2009) or an equivalent model concept such as a dual-permeability model (Stadler et al. 2012), both based on the Richards or two-phase flow equations. Several approaches have been developed to formulate the mass transfer between macropores and matrix domain (Simunek et al. 2003, Gerke 2006, Stadler et al. 2012). It is obvious that the mass transfer is the most crucial part for the mentioned model concepts.

While controlled laboratory experiments with single artificial macropores allow the study of macropore flow and water exchange for specific soils (Edwards et al. 1979, Buttle and Leigh 1997, Ghodrati et al. 1999, Allaire et al. 2002, Castiglione et al. 2003, Köhne and Mohanty 2005, Akay et al. 2008), studies with undistributed soil samples (Bouma et al. 1978) are considerably more complex so that the validation of transfer formulations or the determination of soil specific transfer parameters becomes very complex. Another aspect of verification is that macropore flow and water infiltration on the field scale depend on soil formation, initial conditions and precipitation rates, soil-layers and the coating and lining on the macropore walls (Jarvis 2007).

In this paper we present the model CASCADE which simulates the flow processes in a single vertical macropore and the water exchange between macropore and matrix. The intention was to first investigate and understand macropore infiltration in well-controlled laboratory experiments before later going to large scales. CASCADE was implemented in two existing models for flow in porous media, MUFTE-UG (Helmig et al. 1998) and DuMuX (Flemisch et al. 2011). As the gas phase should be taken into account for complex multi-layered systems (Stadler et al., 2009, 2012) we coupled CASCADE with the two-phase

flow (water, air) module of MUFTE-UG and DuMuX. We compared the numerical results with laboratory infiltration experiments of Germer et al. (2008).

2 MATERIAL AND METHODS

2.1 Laboratory Experiment

The setup presented in Germer et al. 2008 consisted of an artificial macropore placed in a sand-filled half-cylindrical container (Fig. 1). The container was built of stainless steel with a height of 120 cm and a diameter of 100 cm. Openings at a height of 22.5, 37.5, 52.5, 67.5, 82.5 and 97.5 cm allowed the installation of measurement devices inside. A fixed glass pane was placed as section plane so that the infiltration front could be documented with an automated digital camera. A small hole was drilled at the bottom of the container (located in the middle of cylinder) to enable water outflow from the container via the macropore. The soil matrix consisted of fine-textured sand so that the capillary forces caused a high water transfer to the sand.

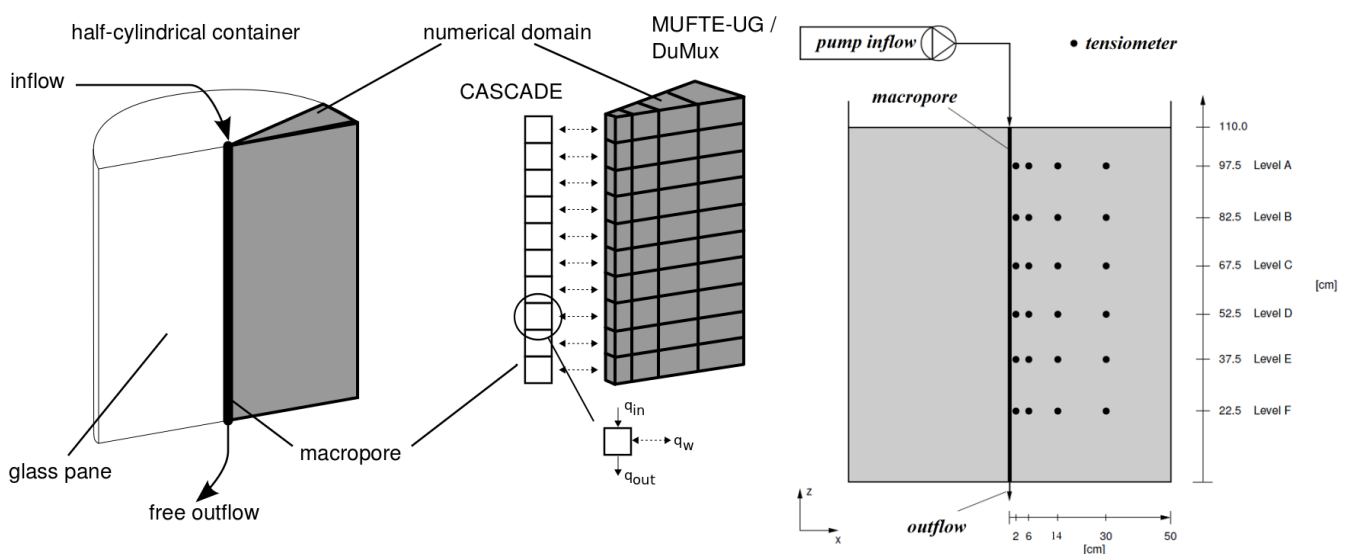


Figure 1. Laboratory infiltration experiment and numerical model: half-cylindrical container (left); numerical domain (middle); measurement devices (right)

Since macropores without a coating are usually not stable in fine sands, an artificial macropore with a diameter of 1 cm and a length of 110 cm was built by a double layer of fine stainless steel wire mesh; the inner mesh of the macropore was coarse for stabilization, while the outer mesh was fine enough to prevent entering of the fine sand. The mesh opening of the outer mesh was equal to the finest grain size of the porous material.

After the macropore was placed in the middle of the container at the glass pane, the lower end was connected with the bottom hole. Then the container was filled step-wise under saturated conditions with sand. Thereby, suction tubes were placed at the bottom after filling the first centimeters, and tensiometers were installed in six heights of the half-cylinder, at each height four openings were used for insertion of four tensiometers with different lengths, so that in one height measurement point in the distance of 2, 6, 14, 30 cm to the macropore were placed (Fig. 1, right). The container was filled as homogeneous as possible up to the height of 110 cm.

The initial conditions for each experiment were established with the suction tubes. The suction at the lower boundary was adjusted to 95 cm, resulting in a capillary head of around 90 cm at the lowest tensiometer level at a height of 22.5 cm. During the infiltration the suction was turned off. A peristaltic pump allowed water injection with a constant flow rate directly into the macropore during the experiment. The infiltration front was recorded by the 24 tensiometers and additional photographs of the infiltration front were taken by an automated digital camera. We used two experiments of Germer et al. (2008) for model validation. The first with a water supply of 166 ml/min (Q166) and an injection time of 484 minutes, the second with a water supply of 375 ml/min (Q375) and an injection time 317 minutes.

2.2 Numerical model

The basic equations for modeling immiscible two-phase flow in porous media are the mass balance equations for both regarded phases α ($w = \text{water}$, $n = \text{air}$) which can be written in a general form as:

$$\frac{\partial(\phi_{\alpha}\rho_{\alpha}S_{\alpha})}{\partial t} + \text{div}(\rho_{\alpha}\underline{v}_{\alpha}) - \rho_{\alpha}q_{\alpha} = 0 \quad (1)$$

where ϕ_{α} (LL^{-3}) is the porosity, S_{α} [-] the saturation of the phase α , ρ_{α} (ML^{-3}) the density, \underline{v}_{α} (LT^{-1}) the Darcy velocity and q_{α} (L^3T^{-1}) a sink/source term. The extended Darcy law is applied to compute the Darcy velocity and it is inserted into the mass balance equations:

$$\underline{v}_{\alpha} = -\mathbf{K} \frac{k_{r\alpha}}{\mu_{\alpha}} (\text{grad } p - \rho_{\alpha} \underline{g}) \quad (2)$$

where \mathbf{K} (L^2) is the intrinsic permeability tensor, $k_{r\alpha}$ (-) the relative permeability, μ_{α} ($\text{ML}^{-1}\text{T}^{-1}$) the determined dynamic viscosity and \underline{g} (MT^{-2}) the vector of gravity. The ratio of relative permeability and dynamic viscosity is called mobility ($\lambda_{\alpha} = k_{r\alpha} / \mu_{\alpha}$). The relative permeability functions after van Genuchten in combination with the Mualem (1976) model are applied.

These mass balance equations build a set of partial differential equations (PDEs). Two primary variables are necessary to solve the non-linear system of equations. Therefore, two supplementary constraints, one for the saturations for the wetting and non-wetting phase ($S_n + S_w = 1$) and one for the capillary pressures p_c ($\text{ML}^{-1}\text{T}^{-2}$) and the phase pressures ($p_c = p_n + p_w$) are required to close the system. The capillary pressure p_c can be described by van Genuchten (1980) as a function of the saturation and soil properties.

The mass transfer between the matrix and macropore domain can be described with different formulations (see also Simunek et al., 2003, Gerke 2006). The formulation chosen here is similar to Darcy's law:

$$u_{\alpha} = -\frac{k_{r\alpha}}{\mu_{\alpha}} \beta (p_{\text{matrix}} - p_{\text{macropore}}) \quad (3)$$

where β (L) is a resistance factor or exchange parameter and controls the flow over the macropore surface. The relative permeability in Eq. (3) is computed with a fully up-winding scheme to prevent unphysical fluxes, assuming a mobility equal to 1 if water infiltrates from the macropore. p_{matrix} ($\text{ML}^{-1}\text{T}^{-2}$) is the water pressure in the matrix and $p_{\text{macropore}}$ ($\text{ML}^{-1}\text{T}^{-2}$) is the water pressure in the macropore which is set to atmospheric pressure. The mass fluxes \dot{m}_{α} (MT^{-1}) between macropore and matrix domain are given as:

$$\dot{m}_{\alpha} = Au_{\alpha}\rho_{\alpha} = q_{\alpha}\rho_{\alpha} \quad (4)$$

where A (L^2) is the surface between matrix and macropore and $\rho_{\alpha}q_{\alpha}$ the sink/source term (see Eq. 1).

CASCADE is implemented as a simple computational scheme to simulate vertical non-capillary macropore flow. Similar model concepts are widely used in hydrology. CASCADE generates for all matrix cells which border to the macropore corresponding CASCADE cells to calculate the cell fluxes with Eq. (4) (Fig. 1, middle). The water exchange between matrix and macropore and vice versa is computed over the whole macropore length and is a source/sink term in the two-phase model of matrix (Eq. 1). Therefore the inflow into the macropore and its value on the top must be known.

Before each time step is carried out with DuMuX or MUFTE-UG, the scheme shifts the infiltrated water cell-wise downwards the macropore; starting at the top and ending at the bottom. Water transfer and downward migration are computed as follows:

- (i) The inflow rate into the macropore at the top is set as boundary condition for the first cell. The water flux based on the pressure difference in both domains (macropore/matrix) is calculated (Eq. 4) for each cell i of CASCADE.
- (ii) Starting from the first cell, lateral water transfer q_w between macropore and matrix is added to (inflow to the macropore) or subtracted from the macropore cell (outflow to the matrix). The vertical outflow q_{out} of a cell serves as input for the next cell (Fig. 1, middle).

$$q_{\text{out},i} = q_{\text{in},i} - q_{w,i} \quad (5)$$

Transfer to the matrix is only calculated as long as enough water is available in the macropore, while water transfer to the macropore can always occur.

- (iii) Remaining water in the macropore at the last cell of CASCADE represents outflow through the macropore bottom.
- (iv) All calculated transfer fluxes are transferred as source/sink terms to the two-phase model of the matrix (Eq. 1).

CASCADE approximates the macropore flow without resolving the flow characteristics inside which are very complex (film flow, plug flow) and cannot be determined in detail. The concept behind CASCADE was chosen to keep the model and the numerical solutions as simple as possible and as accurate as necessary.

The model CASCADE was designed as a flexible extension for existing simulators for flow in porous media. It was written in Python and can be easily coupled with existing models via XML-RPC, embedded Python or exchange files. We tested CASCADE with the numerical toolbox MUFTE-UG (coupling via XML-RPC and embedded Python) and DuMuX (file based coupling).

Both toolboxes apply a local mass conservative box-method for the spatial discretization. The mobility at the integration points is therefore computed with a fully upwinding scheme. A fully implicit adaptive time stepping is used for the discretization in time. The resulting non-linear systems are linearized with the Newton-Raphson method and solved with a BICGstab solver (Helmig et al. 1998, Hinkelmann 2005). Both toolboxes computed the same result, however DuMuX was considerably faster.

3 RESULTS AND DISCUSSION

3.1 Model set-up

We applied a three-dimensional model domain, using the setup symmetry to reduce the domain size and calculation time (see Fig. 1). A mesh with overall 2484 nodes and 1170 elements with a resolution of 46 nodes in the vertical direction is used for simulation. For the given setup it is convenient to use a p_n/S_w formulation. For both phases, we defined Neumann no-flow boundary conditions (BC) on the cylinder surface. At the top we set atmospheric pressure for the gas phase (Dirichlet BC) and a Neumann no-flow BC for the water phase. However, it is also necessary to define a Dirichlet BC for the second primary variable, the water saturation. To minimize the influence of this BC the water saturation was close to the initial condition at the outer edge at the top. The surface between matrix and CASCADE is a crucial part. Here, we chose a Neumann BC for the water phase since the CASCADE model serves as a sink/source term and a Neumann no-flow BC for the gas phase.

3.2 Parameter estimation

A main problem during the study was the determination of the soil hydraulic parameters. The only known parameter for the set-up was the soil porosity ($\phi=0.32$); all other soil hydraulic parameters were fitted during the calibration. In a first step, the capillary pressure was adjusted so that the measured pressure drops (tensiometer) after infiltration was reproduced as good as possible. Then soil parameters (VG_n , VG_α van Genuchten n , α ; K : permeability; β : resistance factor; S_{wr} , S_{wn} : residual water/air saturation) were optimized with the downhill-simplex method (Nocedal and Wright 1999) of Scipy (www.scipy.org). The resulting parameters are given in Tab. 1.

Table 1. Resulting soil parameters

experiment	VG_n [-]	VG_α [Pa^{-1}]	K [m^2]	β [m]	s_{wr} [-]	s_{nr} [-]
Q166	3.75	0.000195	8.19E-12	4.5E-10	0.060	0.020
Q375	5.50	0.000200	7.58E-12	4.5E-10	0.120	0.010

The results of the two different experiments were relatively close together except VG_n . The obtained residual saturations are very small. This is based on the fact that the porosity was very small and the water must be held by the matrix to reproduce the speed of the infiltration front. The quality of the calibration was determined by comparing the measured tensiometer heads with simulated pressures applying the least square method (Fig. 4).

3.3 Infiltration front

The numerical and experimental results are given in Figures 2-4. The photos in Figure 2 show that the fronts were nearly symmetric to the macropore during both experiments. A particular feature of both experimental fronts was the apple-shape; the deepest point of the infiltration front was a few centimeter beside the macropore and not at the macropore itself which can be seen, for example at the front after 30 min. The reason for this behavior was not clear and we could not see this in the numerical results (Fig. 3). The numerical model showed a good agreement of the numerical and experimental infiltration fronts and only for the experiment with the lower infiltration rate (Q166) a small time lag is visible since the simulated front was a little too fast. Later investigations figured out that the packing density in the container increased slightly with depth. Consequently, the model assumption of a homogeneous soil matrix with a constant porosity over depth can be seen as one important factor leading to this discrepancy for low infiltration rates. However, the flow in the matrix had little influence on the water transfer, since water flow only occurred in the upper quarter of the macropore.

The pressure heads h during both infiltrations were measured with the 24 installed tensiometers so that the whole infiltration was tracked (Fig. 4). The tensiometers at the top near the macropore showed an immediate decrease in pressure after the infiltration was started and then remained more or less constant (Fig. 4, left and middle). The water transfer in the upper part of the macropore ($z = 110.0$ cm) had a peak at the beginning and then dropped and remained constant due to the smaller pressure difference between macropore and matrix. The water transfer a bit lower ($z = 95.3$ cm) had nearly the same constant value (Fig. 4, right)

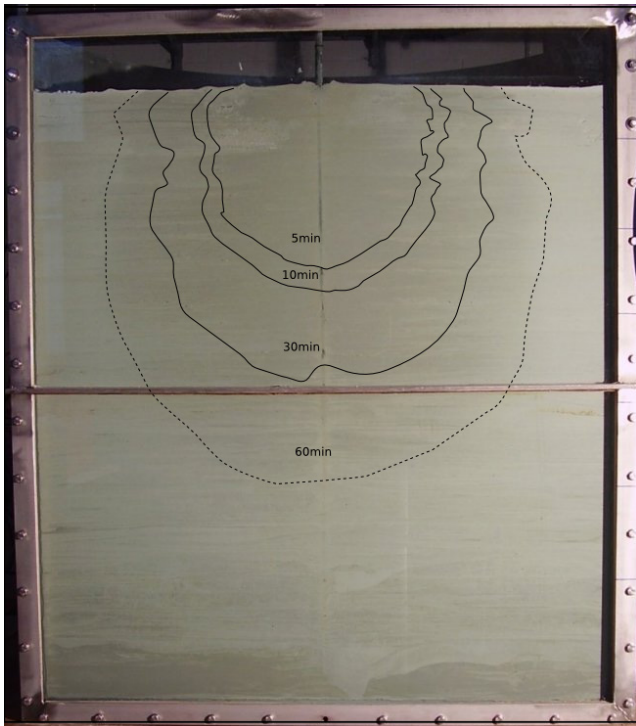


Figure 2. Observed infiltration front of Q166 and Q375 (adopted from Germer 2008)

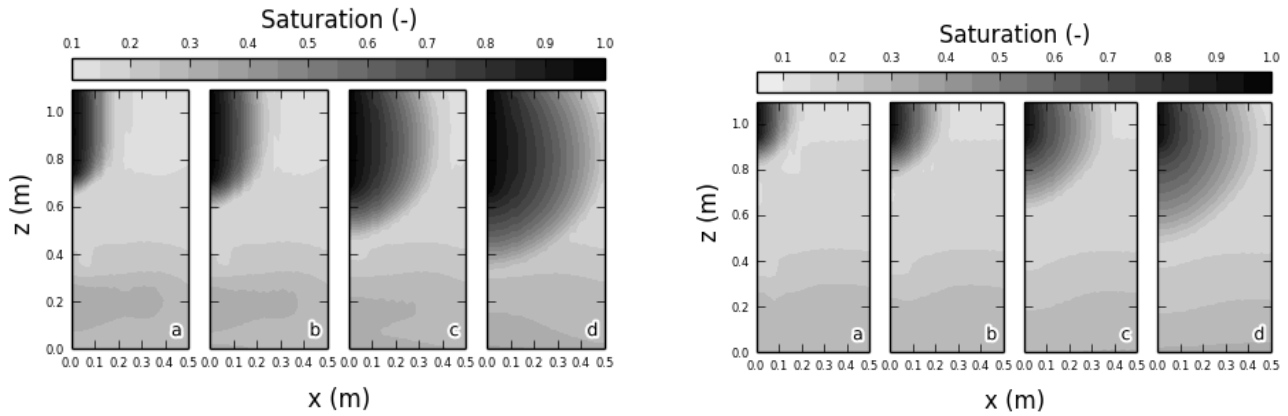


Figure 3. Simulated infiltration front for Q166 (left) and Q375 (right) after 5 min (a), 10 min (b), 30 min (c) and 60 min (d)

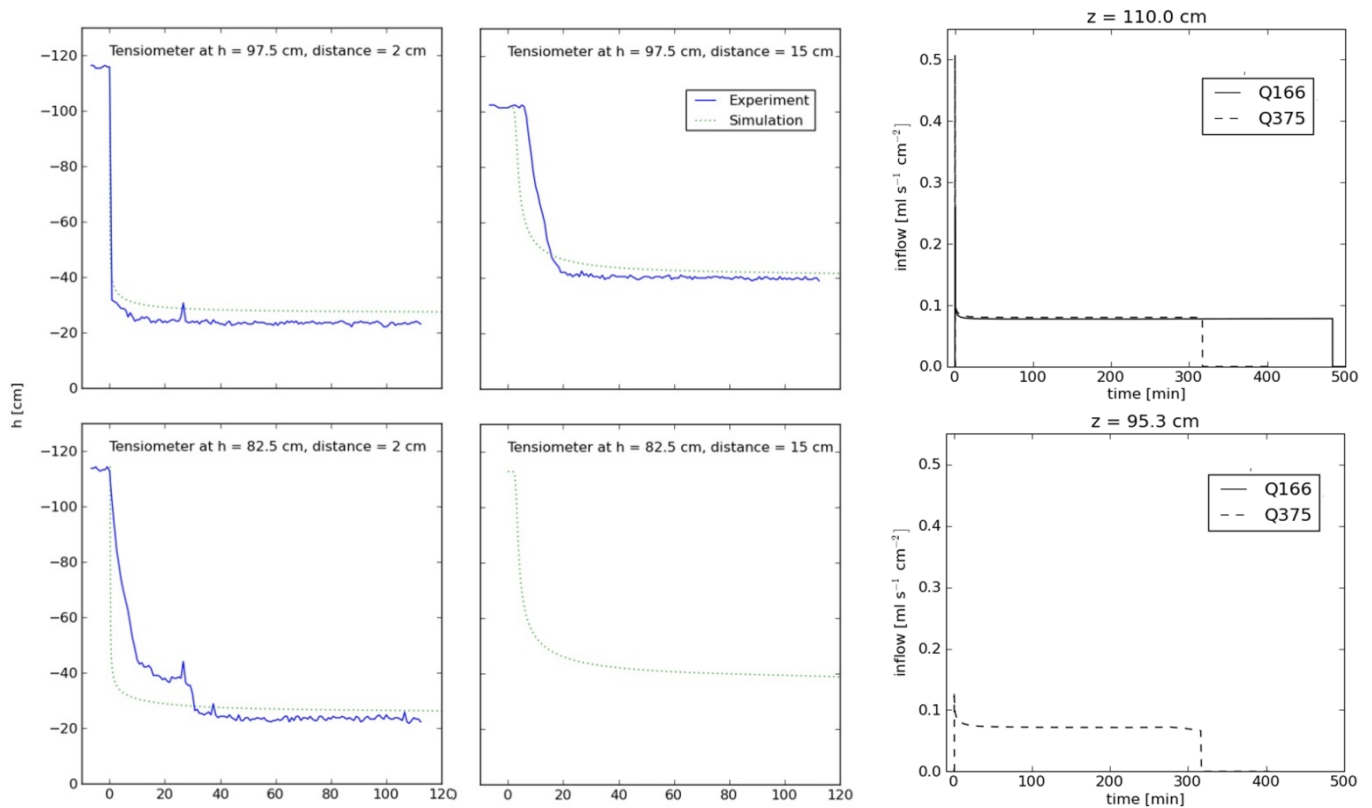


Figure 4. Simulated and measured pressure heads at tensiometers (Q375) at different heights (z) and distances from the macropore: distance 2 cm, $z = 97.5$ cm and 82.5 cm (left); distance 14 cm, $z = 97.5$ cm and 82.5 cm (middle); simulated water exchange between macropore and matrix for Q166 and Q375 (right)

4 CONCLUSIONS

The presented model CASACDE was successfully coupled with two different software packages (MUFTE-UG and DuMuX) to simulate the water infiltration in a single macropore, the water transfer between macropore and matrix and the flow in the soil matrix. In the described cases, the water transfer was dominated by the high capillary suction of the sand matrix. The numerical results showed an overall good agreement with data from laboratory experiments.

ACKNOWLEDGEMENTS

The research was carried out in the Research Unit “Natural Slopes (Großhang) – Coupling of flow and deformation processes for modeling the movement of natural slopes” which was funded by the Deutsche Forschungsgemeinschaft (DFG).

REFERENCES

- Akay O., Fox , G.A., and Simunek, J. (2008). Numerical simulation of flow dynamics during macropore-subsurface drain interactions using HYDRUS. *Vadose Zone J.* 7:909-918.
- Allaire, S.E., Gupta S.C., Nieber, J., and Moncrief, J.F. (2002). Role of macropore continuity and tortuosity on solute transport in soils: 1. Effects of initial and boundary conditions. *J. Contam. Hydrol.* 58:299-321.
- Beven, K.J., and Germann, P. (1982). Macropores and water flow in soils. *Water Resour. Res.* 18:1311-1325.
- Bouma, J., Dekker, L.W. and Wosten, J.H.M. (1978). Case-study on infiltration into dry clay soil. 2. Physical measurements. *Geoderma.* 20:41-51.
- Buttle, J.M., and Leigh, D.G. (1997). The influence of artificial macropores on water and solute transport in laboratory soil columns. *J. Hydrol.* 191:290-313.
- Castiglione, P., Mohanty, B.P., Shouse, P.J., Simunek, J., van Genuchten, M.Th. and Santini, A. (2003). Lateral Water Diffusion in an Artificial Macroporous System: Modeling and Experimental Evidence. *Vadose Zone J.* 2:212-221.
- Edwards, W.M., van der Ploeg, R.R. and Ehlers, W. (1979). A numerical study of the effects of non-capillary-sized pores upon infiltration. *Soil Sci. So. Am. J.* 43:851-856.
- Flemisch, B., Darcis, M., Erbertseder, K., Faigle, B., Lauser, A., Mosthaf, K., Müthing, S., Nuske, P., Tatomir, A., Wolff, M. and Helmig, R. (2011). DuMux: DUNE for Multi-{Phase, Component, Scale, Physics, ...} Flow and Transport in Porous Media. *Advances in Water Resources* 34(9):1102-1112.
- Germer, K., Stadler, L., Hinkelmann, R., Färber, A. and Braun, J. (2008). Studies on Infiltration Processes in a Soil Column with a Single Macropore. Poster at EGU General Assembly, Vienna, Austria.
- Gerke, H.H. (2006). Preferential flow descriptions for structured soils, *J. Plant Nutr. Soil Sci.-Z. Pflanzenernähr. Bodenkd.* 169(3), 382-400.
- Ghodrati, M., Chendorain, M. and Chang, Y.J. (1999). Characterization of macropore flow mechanisms in soil by means of a split macropore column. *Soil Sci. So. Am. J.* 63:1093-1101.
- Helmig, R., Class, H., Huber, R., Sheta, H., Erwig, J., Hinkelmann, R., Jakobs, H. and Bastian, P. (1998). Architecture of the Modular Program System MUFTE-UG for Simulating Multiphase Flow and Transport Processes in Heterogeneous Porous Media, *Mathematische Geologie* 2:123-131.
- Hinkelmann, R. (2005). Efficient Numerical Methods and Information-Processing Techniques for Modeling Hydro- and Environmental Systems. *Lecture Notes in Applied and Computational Mechanics*, Springer.
- Jarvis, N.J. 2007. A review of non-equilibrium water flow and solute transport in soil macropores: principles, controlling factors and consequences for water quality. *European Journal of Soil Sci.* 58:523-546.
- Köhne, J. M., Köhne, S. & Simunek, J. (2009). A review of model applications for structured soils: a) Water flow and tracer transport. *Journal of contaminant hydrology* 104:1-4, 4-35.
- Köhne, J.M., and B. P. Mohanty. (2005). Water flow processes in a soil column with a cylindrical macropore: Experiment and hierarchical modeling. *Water Resour. Res.* 41:W03010. doi:10.1029/2004WR003303.
- Mualem Y. 1976. A new model for predicting the hydraulic conductivity of unsaturated porous media. *Water Resour. Res.* 12:513-522.
- Nocedal, J. and Wright, S. (1999). *Numerical Optimization*, Springer series in operations research and financial engineering, Springer.
- Simunek, J., Jarvis, N.J., van Genuchten, M.T., and Gardenas, A. (2003). Review and comparison of models for describing non-equilibrium and preferential flow and transport in the vadose zone. *J. Hydrol.* 272:14-35.
- Stadler, L., Hinkelmann, R. & Helmig, R. (2012). Modeling Macroporous Soils with a Two-Phase Dual-Permeability Model. *Transport in Porous Media* 95(3):585-601.
- Stadler L., Hinkelmann, R., and Zehe, E. (2009). Two-phase flow simulation of water infiltration into layered natural slopes inducing soil deformation. Editors: Malet, J.-P., A. Remaitre, and T. Bogaard. *Proc. Landslide Processes: From Geomorphologic Mapping to Dynamic Modelling*. CERIG Strassbourg France, pp. 197-201.
- Van Genuchten, M.Th. 1980. A closed-form equation for predicting the hydraulic conductivity of unsaturated soils. *Soil Sci. Soc. Am. J.*, 44:892-898.